

Unidirectional d -wave superconducting domains in the two-dimensional t - J model

Marcin Raczkowski,¹ Manuela Capello,² Didier Poilblanc,² Raymond Frésard,³ and Andrzej M. Oleś^{1,4}

¹*Marian Smoluchowski Institute of Physics, Jagellonian University, Reymonta 4, PL-30059 Kraków, Poland*

²*Laboratoire de Physique Théorique UMR 5152, CNRS and Université Paul Sabatier, F-31062 Toulouse, France*

³*Laboratoire CRISMAT, UMR 6508 CNRS-ENSICAEN, 6 Bld. du Maréchal Juin, F-14050 Caen, France*

⁴*Max-Planck-Institut für Festkörperforschung, Heisenbergstrasse 1, D-70569 Stuttgart, Germany*

(Dated: October 24, 2018)

Motivated by the recently observed pattern of unidirectional domains in high- T_c superconductors [Y. Kohsaka *et al.*, *Science* **315**, 1380 (2007)], we investigate the emergence of spontaneous modulations in the d -wave superconducting resonating valence bond phase using the t - J model at $x = 1/8$ doping. Half-filled charge domains separated by four lattice spacings are found to form along one of the crystal axis leading to modulated superconductivity with *out-of-phase* d -wave order parameters in neighboring domains. Both renormalized mean-field theory and variational Monte Carlo calculations yield that the energies of modulated and uniform phases are very close to each other.

PACS numbers: 74.72.-h, 74.20.Mn, 74.81.-g, 75.40.Mg

Puzzling properties of the high- T_c superconductors have often been attributed to competing instabilities.¹ Indeed, it is believed that doping an antiferromagnetic (AF) Mott insulator (which could be described e.g. by the so-called t - J model²) leads to quantum disordered states with short-ranged magnetic correlations between $S = 1/2$ spins and exotic properties.³ Among them, the resonating valence bond (RVB) state was the first theoretical proposal supposed to capture the essence of high- T_c superconductivity.⁴ Remarkably, this approach based on the Gutzwiller-projected BCS trial wavefunction, the parameters of which are usually determined either by using renormalized mean-field theory⁵ (RMFT) or by variational Monte Carlo (VMC) method,⁶ not only correctly predicted the d -wave symmetry of the superconducting (SC) order parameter,⁷ but reproduced in addition the experimentally observed doping dependence of a variety of physical observables in the SC regime.⁸

In fact, exactly at half-filling where a particle-hole SU(2) symmetry applies, the RVB phase is equivalent to the staggered flux (SF) state,⁹ a projected Slater determinant build from a tight binding model under a staggered magnetic flux. Remarkably, short-ranged staggered orbital current correlations have been seen in the Gutzwiller-projected d -wave RVB phase¹⁰ and in the exact ground state of a small t - J cluster.¹¹ Upon doping the SU(2) symmetry is broken leading to two distinct phases, a d -wave RVB superconductor and a doped SF phase, a candidate for the pseudogap phase,^{12,13} characterized by the opening of an antinodal gap in the excitation spectrum. Indeed, coexistence of sharp nodal quasiparticles and broad antinodal excitations have been found in angle-resolved photoemission spectroscopy (ARPES) studies on an array of underdoped cuprates such as $\text{La}_{2-x}\text{Sr}_x\text{CuO}_4$ (LSCO),¹⁴ $\text{Bi}_2\text{Sr}_2\text{CaCu}_2\text{O}_{8+\delta}$ (Bi2212),¹⁵ and $\text{Ca}_{2-x}\text{Na}_x\text{CuO}_2\text{Cl}_2$ (Na-CCOC).¹⁶

However, there are also some low- T properties of the SC state which cannot be simply explained within the original RVB framework. For example, following its theoretical prediction,¹⁷ static charge and spin stripe or-

der has been detected in neutron scattering experiments and resonant soft x -ray scattering in some cuprate compounds as Nd-LSCO¹⁸ and $\text{La}_{2-x}\text{Ba}_x\text{CuO}_4$ (LBCO).¹⁹ More microscopic evidences of inhomogeneities have been given recently by scanning tunneling microscopy (STM) probing the doped-hole charge density with atomic resolution.²⁰ In the SC regime of two different cuprate families, Na-CCOC and Dy-Bi2212, *bond-centered* charge patterns with a width of four lattice spacings have been seen as well as with two distinct types of spectral gaps: (i) a relatively small one on arrays of two neighboring chains (or “ladder”) with clear coherence peaks as expected for a d -wave superconductor, and (ii) a broader pseudogap-like one on the other separating ladders. This implies inhomogeneous superconductivity across the stripe unit cell. Moreover, spin-glass behavior has been seen in the charge ordered state by muon spin rotation²¹ with a characteristic length of 2 nm, matching perfectly the STM data.²⁰ Also puzzling is the linear vanishing of the density of states at four nodal points that has been observed in the normal phase of LBCO at doping $x = 1/8$.²²

From the above discussion, spatially modulated charge order coexisting either with inhomogeneous AF or SC correlations appears to be ubiquitous among various families of underdoped cuprates. While inhomogeneous AF order was predicted in the “stripe” scenario,¹⁷ SC phase coexisting with charge order is a new fascinating issue. Spatially oscillating d -wave superconductivity appearing on top of an AF stripe modulation has been proposed recently.²³ We provide here a different theoretical proposal based on a RMFT designed to describe *quantum disordered* states²⁴ (no incommensurate AF order is then assumed). Although checkerboard states were first proposed,²⁵ we focus here on modulated SC solutions. Our conclusions are supported by VMC data.²⁶

We start with a t - J model:

$$\mathcal{H} = -t \sum_{\langle ij \rangle, \sigma} (\tilde{c}_{i\sigma}^\dagger \tilde{c}_{j\sigma} + h.c.) + J \sum_{\langle ij \rangle} \mathbf{S}_i \cdot \mathbf{S}_j, \quad (1)$$

where the sums run over the bonds. Next, we replace

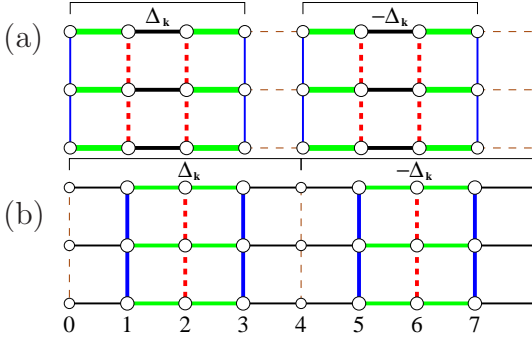


FIG. 1: (color online) Spatial modulation of the hole density n_{hi} (labeled from 0 to 7) found at hole doping $x = 1/8$ and $t/J = 3$ for: (a) *bond-*, and (b) *site-centered* π DRVB configurations. Circle diameters are proportional to the hole densities while widths of bond lines connecting them are proportional to the magnitudes of the pair-order parameter Δ_{ij} .

the local constraints that restrict the fermion creation operators $\tilde{c}_{i\sigma}^\dagger$ to the subspace with no doubly occupied sites by statistical Gutzwiller weights,²⁷ while decoupling in both particle-hole and particle-particle channels yields the following mean-field (MF) Hamiltonian,^{5,28}

$$\begin{aligned} \mathcal{H}_{\text{MF}} = & -t \sum_{\langle ij \rangle, \sigma} g_{ij}^t (c_{i,\sigma}^\dagger c_{j,\sigma} + h.c.) - \mu \sum_{i,\sigma} n_{i,\sigma} \\ & - \frac{3}{4} J \sum_{\langle ij \rangle, \sigma} g_{ij}^J (\chi_{ji} c_{i,\sigma}^\dagger c_{j,\sigma} + h.c. - |\chi_{ij}|^2) \\ & - \frac{3}{4} J \sum_{\langle ij \rangle, \sigma} g_{ij}^J (\Delta_{ji} c_{i,\sigma}^\dagger c_{j,-\sigma}^\dagger + h.c. - |\Delta_{ij}|^2), \quad (2) \end{aligned}$$

with the Bogoliubov-de Gennes self-consistency conditions for the bond- $\chi_{ji} = \langle c_{j,\sigma}^\dagger c_{i,\sigma} \rangle$ and pair-order $\Delta_{ji} = \langle c_{j,-\sigma} c_{i,\sigma} \rangle = \langle c_{i,-\sigma} c_{j,\sigma} \rangle$ parameters in the unprojected state. Moreover, improved Gutzwiller weights depending on local hole densities $n_{hi} = 1 - \sum_{\sigma} \langle c_{i,\sigma}^\dagger c_{i,\sigma} \rangle$ are used,

$$g_{ij}^J = \frac{4(1 - n_{hi})(1 - n_{hj})}{\alpha_{ij} + 8n_{hi}n_{hj}\beta_{ij}^-(2) + 16\beta_{ij}^+(4)}, \quad (3)$$

$$g_{ij}^t = \sqrt{\frac{4n_{hi}n_{hj}(1 - n_{hi})(1 - n_{hj})}{\alpha_{ij} + 8(1 - n_{hi}n_{hj})|\chi_{ij}|^2 + 16|\chi_{ij}|^4}}, \quad (4)$$

with $\alpha_{ij} = (1 - n_{hi}^2)(1 - n_{hj}^2)$ and $\beta_{ij}^\pm(n) = |\Delta_{ij}|^n \pm |\chi_{ij}|^n$, while the $|\chi_{ij}|$ and $|\Delta_{ij}|$ terms account for the correlations of the probabilities between nearest-neighbor sites.²⁸ Using unit cell translation symmetry,²⁹ calculations (with hole doping $x = 1/8$ and $t/J = 3$) were carried out on a large 256×256 cluster at a low temperature $\beta J = 500$ eliminating finite size effects.

The two modulated RVB states derived from the parent d -wave RVB phase found in this study are shown schematically in Fig. 1. Hereafter we refer to them as π -phase domain RVB (π DRVB), as they both involve two out-of-phase SC domains (see also Ref. 23), separated by horizontal/vertical bonds with vanishing pairing amplitudes, named as “domain wall” (DW), where Δ_{ij} gains

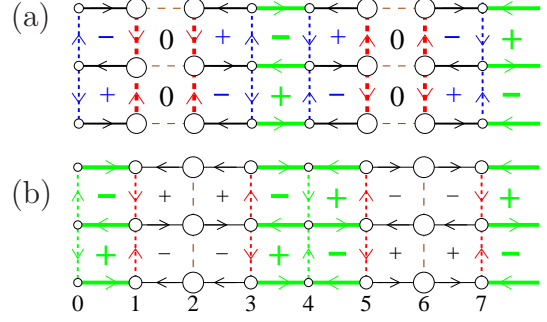


FIG. 2: (color online) Same as in Fig. 1 but for the π DSF patterns. Bond lines with arrows indicate the direction of charge currents and their widths are proportional to the magnitudes of the bond-order parameter χ_{ij} ; $+/-$ symbols refer to positive/negative flux flowing through each plaquette, the magnitude of which is represented by the size of $+/-$ symbol.

a phase shift of π . Specifically, we have found: (i) *bond-centered* π DRVB, with a maximum of the hole density spread over two-leg ladders depicted in Fig. 1(a), and (ii) *site-centered* π DRVB, where the hole rich regions are composed of three-leg ladders as shown in Fig. 1(b). Interestingly, out-of-phase adjacent SC domains has been advocated^{23,30} as responsible for some puzzling decoupling of the CuO_2 planes in stripe-ordered LBCO.³¹

Moreover, as shown in Fig. 2, we also found closely related stripes originating from the SF state. An important characteristic of such patterns (named as π DSF) is again the existence of DWs which (i) act as nodes for the staggered current and (ii) introduce into the SF order parameter a phase shift of π . Hence, the π DSF phase could be regarded as quantum disordered AF stripes.¹⁷ In fact, it differs from the pair density wave checkerboard solution proposed to interpret the pseudogap state,³² not only in terms of the spatial symmetry but also in that it breaks time-reversal symmetry.

Typical profiles of the site- and bond-centered normal π DSF and superconducting π DRVB phases are shown in Fig. 3 and the related MF energies are reported in Table I, compared to VMC estimates.²⁶ Here the locations of the DWs (oriented along the y -axis) of the SC and SF states have been shifted by 2 lattice spacings (exactly as in Figs. 1 and 2) for clarity. Although MF results are mostly qualitative, as they are exact for particular small clusters only,³³ they are believed to correctly reflect the local spatial structure of the various states, in particular the out-of-phase nature of the respective order parameters $\Delta_{i\alpha}^{\text{SC}} = g_{i,i+\alpha}^t \Delta_{i,i+\alpha}$ and *modulated* flux $\Phi_{\pi i}$ ³⁴ in neighboring domains as shown in Figs. 3(c,d). The hole density profiles in the bond-centered (site-centered) stripes show the emergence of two (three) inequivalent sites in the unit cell. One important feature of these DWs is that they are half-filled, i.e. the integrated charge density in the direction perpendicular to the DWs corresponds to an average of one hole every eight sites. Although the large quantitative differences between the magnitudes of the charge modulations (as well

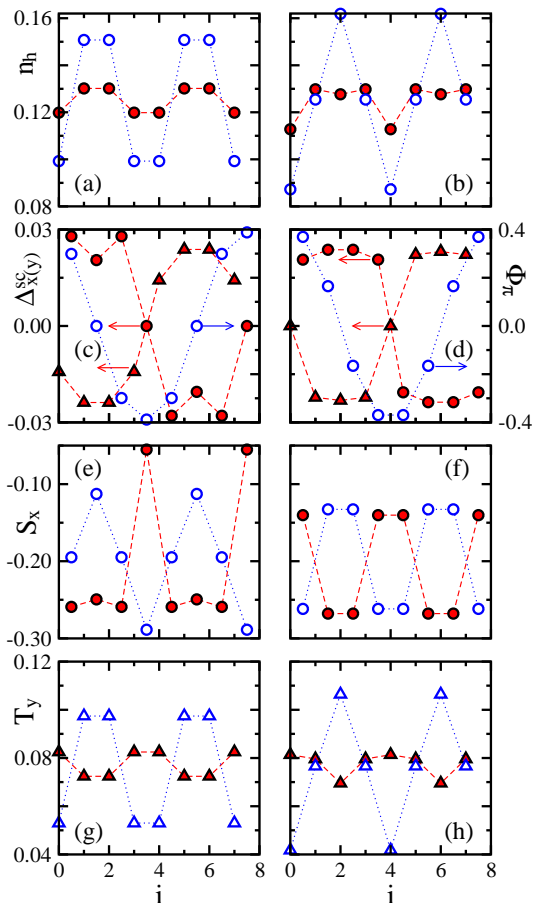


FIG. 3: (color online) (a,b) Hole density n_{hi} , (c,d) SC order parameter $\Delta_{i\alpha}^{SC}$ / modulated flux $\Phi_{\pi i}$ indicated by left/right arrows, (e,f) spin correlation S_i^x , and (g,h) bond charge T_i^y , found in the π DSF (open symbols) and π DRVB (filled symbols) phase. Left (right) panels depict *bond-* (*site-centered*) pattern; circles (triangles) in panels (c-h) correspond to the x (y) direction, respectively.

as their opposite signs) in the superconducting and normal states might be an artefact of the Gutzwiller/mean-field approximations,²⁶ the generic trend towards charge segregation clearly reflects the competition between the superexchange energy (E_J) and the kinetic energy (E_t) of doped holes. For example, a reduction of the SC or flux order parameters (the latter known to frustrate coherent hole motion¹³) enables a large bond charge hopping $T_i^y = 2g_{i,i+y}^t Re\{\chi_{i,i+y}\}$ along the DWs, as in the usual stripe scenario,^{17,29} at the expense of a reduction of the AF correlations $S_i^x = -\frac{3}{2}g_{i,i+x}^J (|\chi_{i,i+x}|^2 + |\Delta_{i,i+x}|^2)$ along the transverse bonds. Although earlier VMC studies³⁵ suggested that the d -wave RVB state has a lesser tendency towards phase separation than the SF, our results (including the VMC results²⁶ of Table I) clearly demonstrate that the modulated phases with commensurate period $\lambda = 8$ (at $x = 1/8$) are very competitive in energy with the homogeneous ones.³⁶ Hence, under some circumstances, such as long-ranged Coulomb repulsion²⁵ or in-plane anisotropy, the d -wave stripe ordered phase

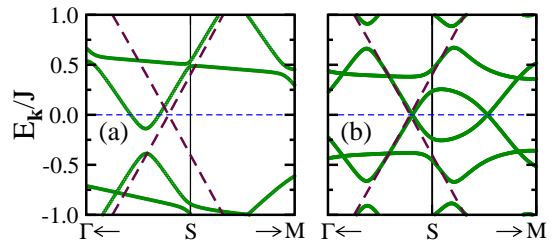


FIG. 4: (color online) MF spectrum $E_{\mathbf{k}}$ of: (a) π DSF phase and (b) π DRVB phase along the nodal $\Gamma - M$ path *near* the S point. Dashed line shows $E_{\mathbf{k}}$ of the d -wave RVB phase.

might correspond to the global minimum as suggested by the experimental data for Nd-LSCO,¹⁸ LBCO,¹⁹ and Na-CCOC,²⁰ all with a tetragonal structural distortion. In addition, the reinforcement of the short-ranged AF correlations by the finite flux flowing through plaquettes of weakly doped regions in the π DSF phase helps to optimize E_J . Consequently, such a phase is characterized by a better E_J as compared to the uniform SF state (see Table I). Hence an increased tendency of the latter towards phase separation should result from increasing J or reducing x , in which case the kinetic energy gain is relatively unimportant.

It is instructive to investigate the low-energy part of the MF spectrum $E_{\mathbf{k}}$ (see Fig. 4) which may reflect interesting features of the true quasiparticle spectrum. It is well known that the uniform SF phase has a cone-like dispersion pinned at the $S = (\pi/2, \pi/2)$ point. However, doping pushes the node above the chemical potential leading to small “pockets” and it has been recently shown that a diagonal π DSF phase follows the same trend.³⁴ In contrast, since the vertical π DSF state mixes currents with different chiralities, one finds two cone-like features located symmetrically around the S point. However, only one of them crosses the chemical potential which may lead to small electronic pockets weakly shifted towards the Brillouin zone (BZ) center. They are reminiscent of the electron pockets obtained in a recent slave boson study of the $t - t' - U$ Hubbard model.³⁷ Interestingly, the parent d -wave RVB phase and its modulated π DRVB derivate both show a cone-like linear quasiparticle exci-

TABLE I: MF kinetic energy E_t , magnetic energy E_J , and free energy F as well as VMC energy E_{VMC} for a tilted cluster of 128 sites of the locally stable phases (all per site): π DSF, SF, *bond-centered* π DRVB(1), *site-centered* π DRVB(2), and d -wave RVB one. π DSF(1) and π DSF(2) phases are fully degenerate.

phase	E_t/J	E_J/J	F/J	E_{VMC}/J
π DSF	-0.8514	-0.4269	-1.2783	-1.3323
SF	-0.8622	-0.4230	-1.2852	-1.3389
π DRVB(2)	-0.8736	-0.4491	-1.3227	-1.3359
π DRVB(1)	-0.8719	-0.4518	-1.3237	-1.3359
d -wave RVB	-0.8863	-0.4784	-1.3647	-1.3671

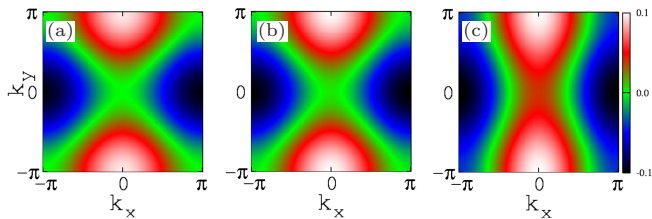


FIG. 5: (Color) Real part of the SC order parameter $\Delta_{\mathbf{k}}^{\text{SC}}(\mathbf{Q})$ in: (a) d -wave RVB phase with $\mathbf{Q} = (0, 0)$ as well as in the *bond-centered* π DRV B phase with: (b) $\mathbf{Q} = \pm(\pi/4, 0)$ and (c) $\mathbf{Q} = \pm(3\pi/4, 0)$ (scaled resp. by factors 4.5 and 8 for clarity).

tation spectrum pinned at the chemical potential at a location in the BZ close to the cone of the vertical π DSF phase. We also note that the presence of DWs induces the formation of a flat band in the vicinity of the antinodal direction that could be related to the ARPES observation in underdoped cuprates.^{14,15,16}

Lastly, in Figs. 5(a,b) we compare the (double) Fourier transform of the SC order parameter $\Delta_{\mathbf{k}}^{\text{SC}}(\mathbf{Q}) = \frac{1}{N} \sum_{\langle ij \rangle} e^{i\mathbf{Q}\cdot\mathbf{R}_i + i(\mathbf{k}-\mathbf{Q}/2)\cdot(\mathbf{R}_i-\mathbf{R}_j)} \Delta_{ij}^{\text{SC}}$ to the uniform RVB SC gap. At the Cooper pair momenta $\mathbf{Q} = \pm(\pi/4, 0)$ both real and imaginary parts (not shown) of $\Delta_{\mathbf{k}}^{\text{SC}}(\mathbf{Q})$ retain much of the d -wave symmetry with a gap close to the nodal directions. Moreover, in contrast to Ref. 23, $\Delta_{\mathbf{k}}^{\text{SC}}(\mathbf{Q})$ is also non-vanishing in the π DRV B phase for

$\mathbf{Q} = \pm(3\pi/4, 0)$. Of lower amplitude the latter clearly reflects the DW structure through its deviation from d -wave symmetry, as seen in Fig. 5(c).

To conclude, we note that the relative stability of the modulated d -wave RVB superconductor should be highly sensitive to small perturbations of the microscopic Hamiltonian and, hence, can be relevant to some experimental cases such as the bond-centered electronic glass with unidirectional DWs in Na-CCOC and Dy-Bi2212 seen by STM.²⁰ In fact, an experimental support to our modulated bond-centered superconducting state is provided by its strong similarities to the experimental pattern indicating the spontaneous appearance of two types of parallel ladders on nano-domains.²⁰

Acknowledgments

We thank J. C. Davis and J. M. Tranquada for helpful correspondence. M. Raczkowski acknowledges support from the Foundation for Polish Science (FNP) and thanks the Laboratoires CRISMAT in Caen and IRSAMC in Toulouse for hospitality. This research was supported by the Polish Ministry of Science and Education under Project No. N202 068 32/1481. M. Capello thanks the Agence Nationale de la Recherche (France) for support.

¹ M. Vojta, Y. Zhang, and S. Sachdev, Phys. Rev. B **62**, 6721 (2000).
² K. A. Chao, J. Spalek, and A. M. Oleś, J. Phys. C **10**, L271 (1977); Phys. Rev. B **18**, 3453 (1978); F. C. Zhang and T. M. Rice, *ibid.* **37**, 3759 (1988).
³ S. Sachdev, Rev. Mod. Phys. **75**, 913 (2003).
⁴ P. W. Anderson, Science **235**, 1196 (1987).
⁵ F. C. Zhang *et al.*, Supercond. Sci. Technol. **1**, 36 (1988).
⁶ C. Gros, Phys. Rev. B **38**, 931 (1988); S. Sorella *et al.*, Phys. Rev. Lett. **88**, 117002 (2002).
⁷ G. Kotliar and J. Liu, Phys. Rev. B **38**, 5142 (1988).
⁸ M. Calandra and S. Sorella, Phys. Rev. B **61**, R11894 (2000); P. W. Anderson *et al.*, J. Phys. Condens. Matter **16**, R755 (2004).
⁹ I. Affleck and J. B. Marston, Phys. Rev. B **37**, R3774 (1988).
¹⁰ D. A. Ivanov, P. A. Lee, and X.-G. Wen, Phys. Rev. Lett. **84**, 3958 (2000).
¹¹ P. W. Leung, Phys. Rev. B **62**, R6112 (2000).
¹² S. Chakravarty *et al.*, Phys. Rev. B **63**, 094503 (2001).
¹³ For numerical computations of doped SF see, e. g., D. Poilblanc and Y. Hasegawa, Phys. Rev. B **41**, 6989 (1990); T. K. Lee and L. N. Chang, *ibid.* **42**, 8720 (1990).
¹⁴ M. Hashimoto *et al.*, Phys. Rev. B **75**, 140503(R) (2007).
¹⁵ K. Tanaka *et al.*, Science **314**, 1910 (2006).
¹⁶ K. M. Shen *et al.*, Science **307**, 901 (2005).
¹⁷ J. Zaanen and O. Gunnarsson, Phys. Rev. B **40**, 7391 (1989); D. Poilblanc and T. M. Rice, *ibid.* **39**, 9749 (1989); K. Machida, Physica C **158**, 192 (1989).
¹⁸ J. M. Tranquada *et al.*, Nature (London) **375**, 561 (1995);

N. Christensen *et al.*, Phys. Rev. Lett. **98**, 197003 (2007).
¹⁹ M. Fujita *et al.*, Phys. Rev. B **70**, 104517 (2004); P. Abamonte *et al.*, Nature Physics **1**, 155 (2005).
²⁰ Y. Kohsaka *et al.*, Science **315**, 1380 (2007); see also J. Zaanen, *ibid.* **315**, 1372 (2007).
²¹ K. Ohishi *et al.*, J. Phys. Soc. Jpn. **74**, 2408 (2005).
²² T. Valla *et al.*, Science **314**, 1914 (2006).
²³ A. Himeda, T. Kato and M. Ogata, Phys. Rev. Lett. **88**, 117001 (2002); note that here a single sinusoidal modulation was assumed.
²⁴ M. Vojta, Phys. Rev. B **66**, 104505 (2002).
²⁵ H.-X. Huang, Y.-Q. Li, and F. C. Zhang, Phys. Rev. B **71**, 184514 (2005); D. Poilblanc, *ibid.* **72**, 060508(R) (2005); C. Weber *et al.*, *ibid.* **74**, 104506 (2006).
²⁶ The VMC results will be presented in detail elsewhere.
²⁷ D. Vollhardt, Rev. Mod. Phys. **56**, 99 (1984).
²⁸ M. Sigrist *et al.*, Phys. Rev. B **49**, 12058 (1994).
²⁹ M. Raczkowski, R. Frésard, and A. M. Oleś, Phys. Rev. B **73**, 174525 (2006); Europhys. Lett. **76**, 128 (2006).
³⁰ E. Berg *et al.*, Phys. Rev. Lett. **99**, 127003 (2007).
³¹ Q. Li *et al.*, Phys. Rev. Lett. **99**, 067001 (2007).
³² H.-D. Chen *et al.*, Phys. Rev. Lett. **93**, 187002 (2004).
³³ R. Frésard, H. Ouerdane, and T. Kopp, (unpublished).
³⁴ M. Raczkowski *et al.*, Phys. Rev. B **75**, 094505 (2007).
³⁵ D. A. Ivanov, Phys. Rev. B **70**, 104503 (2004).
³⁶ Jastrow factors can lead to slightly lower energies and to a change in the ranking of the various states, see Ref. 26.
³⁷ M. Raczkowski *et al.*, Phys. stat. sol. (b) **244**, 2521 (2007).